MC-NG: A 4th GENERATION SINGLE-CRYSTAL SUPERALLOY FOR FUTURE AERONAUTICAL TURBINE BLADES AND VANES

Didier Argence*, Cyril Vernault**, Yves Desvallées* and Dominique Fournier**

*SNECMA, Materials and Processing Department, Villaroche center 77556 Moissy-Cramayel Cedex, France
**TURBOMECA, Materials and Coatings Department, 64511 Bordes Cedex, France

Abstract

The growing demand for an increasing turbine inlet temperature has led both French engine manufacturers Snecma and Turbomeca to take into account the attractive potential of alloys containing rhenium and ruthenium. The MC-NG is a 4th generation single-crystal superalloy developed and patented by Onera.

This paper discusses both microstructural aspects and mechanical properties obtained on the first MC-NG alloy elaborated in industrial conditions. Results demonstrate that there is a promising alternative to the third generation superalloys to increase the temperature capability of the single-crystal turbine blades without the drawback of a too high density or microstructural instability features.

Introduction

It is clearly established and fully documented that aeronautical turbine blades are submitted to creep and fatigue at high temperature. In such conditions fatigue and creep tests performed in laboratories have shown that grain boundaries constitute preferential sites for crack initiation and propagation. Hence, the continuous need for an increasing turbine inlet temperature has led engine manufacturers to use materials which have a low intergranular sensibility.

Considering this context and including casting progress in directional solidification, gas turbine manufacturers who used, in the past, cast polycrystalline superalloys have moved towards columnar structures and finally single crystals. By developing nickel base superalloy chemistries, alloy designers have largely contributed to the improvement of high temperature mechanical properties of this kind of materials. As a result, the latest single-crystal superalloys constitute the 4th generation. This new alloys family is characterised by high rhenium and ruthenium contents. These alloying elements were indeed shown to have a strong beneficial effect on the long-term microstructural destabilisation especially during high temperature creep.

Currently, calculations for future engine programs based on behaviour and damage laws obtained for single crystals in service (AM1, AM3 and MC2 used for the M88 Rafale fighter's engine or Arriel 2 and Arrius 2 for Eurocopter and Sikorsky helicopter applications) show the advantages of the new single-crystal generation.

For both French engine manufacturers Snecma and Turbomeca, these new objectives can be reached with the manufacturing of MC-NG (Mono Cristal – Nouvelle Génération) blades which are intended for commercial and military engines. The MC-NG is a single-crystal superalloy developed and patented by Onera [1]. Before being used for operating engines, it is necessary to fully characterise the single crystal superalloy in order to obtain the basic properties and to identify its behaviour laws and damage models.

This paper deals with preliminary results regarding metallurgical characteristics, mechanical and oxidation-corrosion properties obtained on the first MC-NG alloy elaborated in industrial conditions.

Metallurgical study

As-cast material and solutioning treatment analysis

The composition and density of MC-NG are indicated in Table I together with chemical compositions and densities of AM1, AM3, MC2 and CMSX-4 alloys. It is to be noted that first (AM1 and AM3) and second (MC2) single-crystal generations are composed of rather similar elements whereas MC-NG exhibits an innovative composition with rhenium and ruthenium contents. Since these elements are relatively heavy, MC-NG density is higher than current single-crystal alloys, but as the same level of density than CMSX-4.

Furthermore, some differences in microstructure of the as-cast material can be expected in MC-NG as compared to AM1, AM3 and MC2. A metallurgical study on small bars of 10 and 14 mm diameter allowed us to quantify the eutectic content, by using an image analysis method. This method consists in examining 50 non-consecutive fields at a magnification of 250. The average fraction of eutectic phase counted on MC-NG is 2.8%. As compared to AM1 alloy (3%) the eutectic percentage is similar.

An other target set for the as-cast MC-NG alloy study was to determine the aspect and the size of the gamma prime phase. Two populations of γ' can be observed. The first one is located inside inter-dendritic areas where precipitates exhibit a square or circular features and a size in the range 0.6 – 0.7 µm (Figure 1). Furthermore, in dendrite's bulk, γ' looks like squares or stars of around 0.5 µm (Figure 2). However, a similar aspect has already been observed on current single crystals.

The definition of the solution treatment depends also on the burning temperature of the alloy. Hence, isothermal burning tests were performed on MC-NG at intervals of 10°C between 1310°C and 1360°C for 1 hour. Few burn points appeared at 1340°C. After a new test at 1335°C, the burning temperature of the MC-NG alloy has been ultimately defined at 1340°C. Quantitative studies on eutectic content and burning tests justify that the MC-NG superalloy solution treatment consist of a 10-hour dwell time at 1340°C (close to the CMSX-10 superalloy solution treatment) after a very slow rate heating (3°C per hour) between 1310°C and 1340°C. Indeed, this heat treatment is necessary to remove all the eutectic phases and to homogenise the material. It is to be noticed that the solution treatment is longer than on current single crystals since the dwell time is only 3 hours at 1300°C for AM1, AM3 and MC2 superalloys.

Table I Chemical compositions and densities of considered single-crystal superalloys

Alloy	Cr	Co	Mo	W	Ta	Re	Ru	Al	Ti	Hf	Ni	Density
AM1	8	6	2	6	9	-	-	5.2	1.2	-	bal	8.6
AM3	8	5.5	2.2	5	3.5	-	-	6	2	-	bal	8.25
MC2	8	5	2	8	6	-	-	5	1.5	-	bal	8.63
CMSX-4	6.5	9	0.6	6	6.5	3	-	5.6	1	0.1	bal	8.7
MC-NG†	4	<0.2	1	5	5	4	4	6	0.5	0.1	bal	8.75

†: MC-NG data correspond to the MC-NG 544 grade elaborated and patented by Onera.

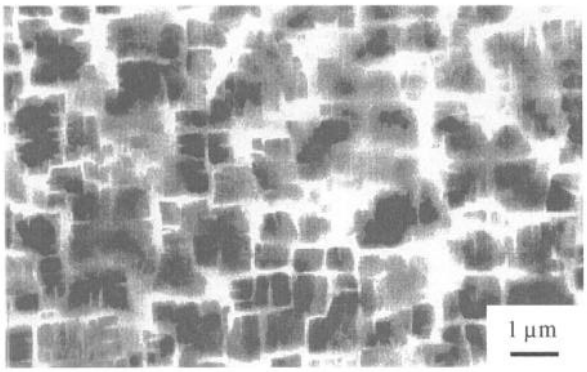

Figure 1: γ' aspect inside inter-dendritic zone.

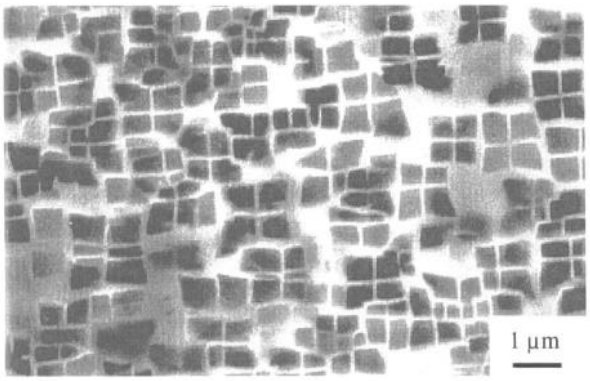

Figure 2: γ' aspect in dendrite's bulk.

Ageing treatment definition

Different heat treatments were applied in order to define the optimum conditions to provide expected the mechanical properties. Since it is necessary to use coatings in service, the considered ageing treatment, consists of two successive thermal treatments; the first one is aimed at ensuring coating diffusion whereas the second one stabilises the microstructure of the alloy.

Moreover, a brazing heat treatment simulation has also been considered. Table II synthesizes all explored conditions.

For each condition, the tensile properties at 750°C and γ' size were determined in order to choose the adequate ageing treatment.

The results are also indicated in Table II.

Tensile tests reveal the important role of the stabilising treatment (R2). For instance, reducing the dwell time from 16 hours to 4 hours significantly decreases the mechanical resistance.

A secondary role can be attributed to the primary γ' size. For instance, the increase of their size induces an improvement of tensile strength. Nevertheless, this effect disappears when the stabilising treatment duration is sufficient (16 hours). Even if it is not evidenced, the drastic effect of the stabilising dwell time is supposed to be partly due to a secondary γ' phase precipitation.

It ought to also be noted that the brazing heat treatment simulation does not modify the tensile properties of MC-NG alloy at 750°C. Hence, the thermal treatment sequence 1100°C/4hrs + 870°C/16 hrs has been chosen as the basic one.

In addition to defined conditions for obtaining a fully heat-treated alloy, the influence of heat treatment on microstructure stability was analysed. It appears that the γ' phase in MC-NG is less sensitive to a dwell time at very high temperature (1225°C) than in AM3 and MC2 alloys. While γ' precipitates are solution-treated for current single crystals (AM3, MC2), their aspect and distribution in MC-NG are nearly unchanged at this temperature. This behaviour must be correlated to the presence of alloying elements Re and Ru which reinforce the γ' phase. As a consequence, an improvement of the mechanical properties at high temperature is expected.

Table II MC-NG heat-treatment conditions explored and associated tensile properties at 750°C

Heat treatment	Brazing treatment (B)	Diffusion treatment (R1)	Stabilisation treatment (R2)	Ultimate Tensile Stress (MPa)	Yield Stress (MPa)	Elongation A%	γ' size (µm)
N° 1	-	1100°C/4 hrs	870°C/4 hrs	1038	809	11.6	540
N° 2	-	1150°C/4 hrs	870°C/4 hrs	1054	826	13.2	610
N° 3	-	1100°C/7 hrs	870°C/4 hrs	1044	818	12.4	640
N° 4	-	1100°C/4 hrs	870°C/16 hrs	1225	915	7.7	550
N° 5	-	1150°C/4 hrs	870°C/16 hrs	1105	827	10.2	700
N° 6	1220°C/23 min	1100°C/4 hrs	870°C/16 hrs	1191	904	7.3	720

Mechanical properties

Mechanical properties of MC-NG superalloy have been characterised though tensile, creep and low-cycle fatigue tests. Specimens were machined from fully heat-treated bars of 14 mm diameter. The disorientation between the <001> axis of the crystal and the test bar axis was, in all cases, less than 10 degrees.

Tensile properties

Tensile tests were performed on smooth samples from room temperature up to 1150°C. Figure 3 represents the ultimate tensile stress and the yield stress as a function of temperature.

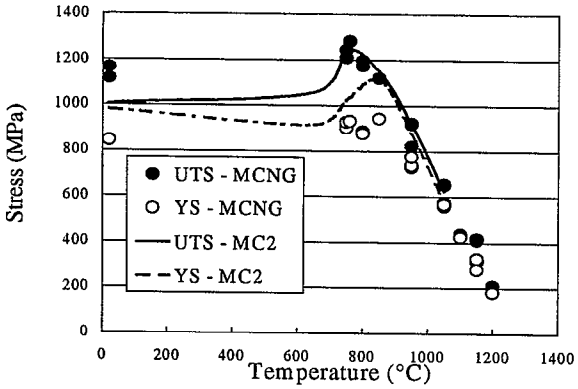

Figure 3: Tensile properties as a function of temperature.

Roughly tensile data are above current single-crystal data up to 1150°C. Only the yield strength is slightly below between room temperature and 800°C. This behaviour is not yet understood.

Creep properties

Creep tests were performed in the temperature range of 900°C to 1200°C. Since a Larson-Miller diagram does not allow the illustration of all test conditions when controlling strain or when damage mode is changed, MC-NG creep strength is represented in two figures. The first one shows a classic Larson-Miller curve where all test results obtained up to 1150°C are collected (Figure 4).

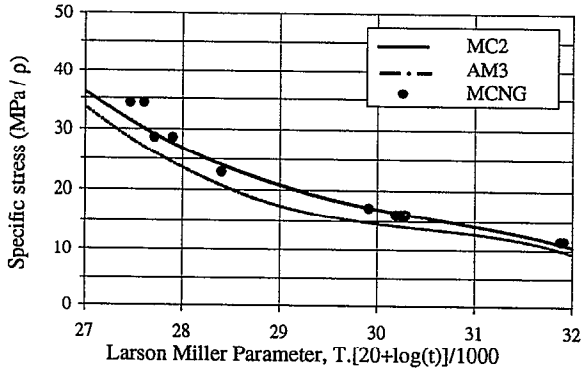

Figure 4: Creep-rupture results - Larson – Miller diagram.

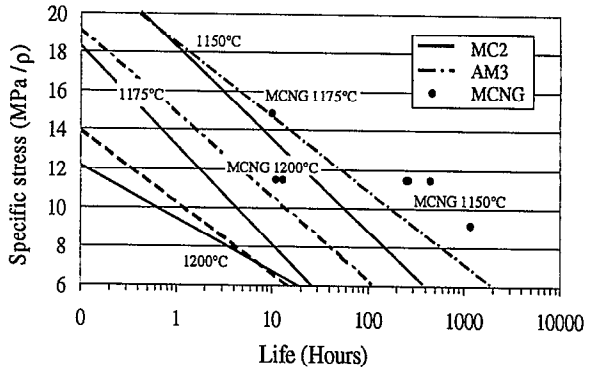

Figure 5: Creep results – time to rupture as a function of temperature.

Indeed this temperature was identified to be the transition between two behaviour modes. Figure 5 illustrates, for different temperatures, times to rupture as a function of the density normalised specific stress.

Considering both figures it can be concluded that the MC-NG creep strength is remarkable. In a large range of temperatures, the average time to rupture of this alloy is higher than on current single crystals. This difference is even more important for medium (~ 900°C) and very high temperatures (≥ 1150°C). For instance at 1200°C, improvements by a factor 25 and 60 on creep rupture times are observed in comparison with AM3 and MC2 alloys respectively. However, MC2 remains the reference material for creep properties in the temperature range of 1000°C-1050°C.

The significant higher creep resistance of MC-NG for temperatures above 1150°C can be explained by the increase of the residual fraction of γ' phase in this temperature range as compared to the case of MC2. This behaviour has been previously discussed in this paper, in terms of the delaying effect on microstructural destabilisation associated to the Re and Ru presence.

Low-cycle fatigue properties

Cyclic tests were carried out under different levels of stress amplitude at 950°C and 1100°C. Low-cycle fatigue tests were performed with and without dwell time (trapezoid cycle 10-90-10 or sinusoidal cycle at 0.5 Hz).

Figure 6 illustrates the MC-NG number of cycles to failure as a function of the normalised stress amplitude for all fatigue tests. Open symbols represent tests with dwell time at both temperatures. Comparable published data on AM1 alloys [2] are included.

Considering pure low cycle fatigue at 950°C, it appears that MC-NG properties are very promising. For instance, an improvement by a factor 6 on the fatigue life is observed in comparison with AM1.

Introducing a dwell time during cycling induces a decrease of the fatigue strength. This negative effect is equivalent for both test temperatures and roughly represents a factor 40 on the number of cycles to failure.

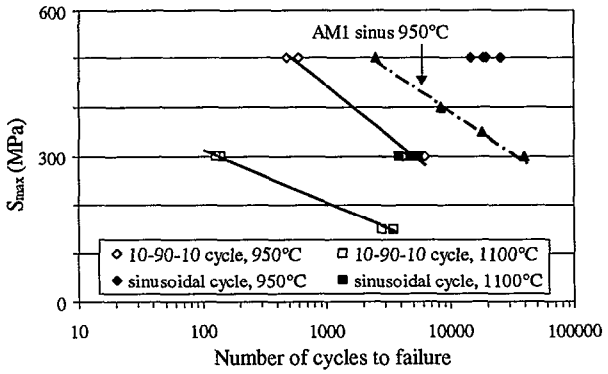

Figure 6: MC-NG low-cycle fatigue results – Number of cycles to failure as a function of normalised stress amplitude.

SEM analyses of fracture surfaces have shown, for tests performed without dwell time, that fatigue damage mechanisms are different for both test temperatures.
Indeed at 950°C, only one microcrack initiates on a subsurface shrinkage and leads to failure. On the contrary, at 1100°C, even if the thick oxide layer on the fracture surface does not allow the identification of initiation sites, the specimens' surface exhibits numerous uniformly distributed cracks.
As regard fatigue tests with dwell time, numerous cracks are also observed on samples' surface. Microcracks are initiated from the thick superficial oxide layer.
For both temperatures 950°C and 1100°C, microstructural investigations carried out from fracture area show the formation of a typical raft structure. This structure appears to be more evident at higher temperature.
Furthermore, observations of the specimens' longitudinal sections reveal the large population of micropores aligned along interdendritic spaces. Such behaviour is associated with creep damage during dwell time.

Environmental effect and microstructural stability

The behaviour of MC-NG in relation to environment has been investigated with air oxidation and sulfidation corrosion experiments under cyclic temperature. In order to prevent the damage development, the specimens were coated with a protective layer. This layer also plays the role of bondcoat for the thermal barrier coating. However the protection can induce the formation of a Secondary Reaction Zone (SRZ) within the underlying material [3,4]. This zone contains plate-like shaped Topologically Closed Packed (TCP) precipitates which could affect the mechanical properties [5,6].

Oxidation resistance

Several cyclic oxidation tests with a dwell time at 1100°C were performed on uncoated AM1 and MC-NG specimens. The classic curve of mass evolution (denoted Δm) is shown in Figure 7:

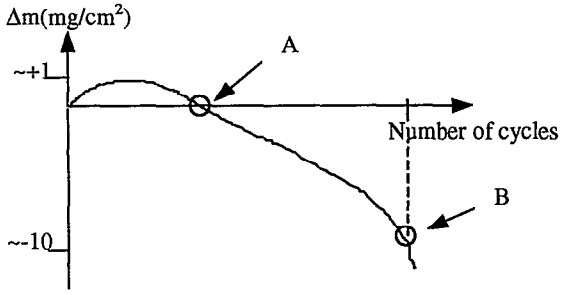

Figure 7: Standard curve of mass evolution during oxidation test.

At the beginning of the test, the specimen weight increases which is progressively balanced by scaling of the oxidation layer. The A (Δm=0) and B (Δm=-10) values are used for data analysis. They allow the comparison of the specimen oxidation resistance. Below -10mg/cm^2 we consider that the oxide is entirely spalled. The tests performed on uncoated specimens show that the MC-NG is clearly more resistant to oxidation than AM1 (Table III). For the same number of cycles the mass reduction of AM1 is close to -10mg/cm^2 while it is still positive for MC-NG.

Table III Oxidation resistance of uncoated AM1 and MC-NG specimens

Alloy	Δm=0 mg/cm^2 (number of cycles)	Δm=-10 mg/cm^2 (number of cycles)
AM1	150	500
MC-NG	400	>1300

This difference of oxidation behaviour can be explained by the beneficial influence of alloying elements like rhenium and ruthenium which are present in the MC-NG alloy. However, other studies have shown that the difference is strongly linked with the alloy cleanness and particularly to the segregating elements which inhibit oxide scale adhesion [7,8].

Corrosion resistance

Snecma carried out several cyclic corrosion tests, at 850-900°C, on uncoated AM1 and MC-NG specimens.
During the 45 minute dwell time, a salt mist is introduced in the chamber with kerosene to obtain specific conditions (1mg/cm^2 of Na_2SO_4 for 100h exposure). For the data analysis, the number of cycles to initiation (pits) and to complete corrosion of the surface are counted. The results (Table IV) show that the corrosion resistance of MC-NG is better than the AM1 one.

Table IV Corrosion resistance of uncoated AM1 and MC-NG specimens

Alloy	Initiation (number of cycles)	End (number of cycles)
AM1	30-50	100-150
MC-NG	140-240	200-300

The intrinsic corrosion resistance of MC-NG was also investigated by Turbomeca with other cyclic corrosion tests at 900°C. Results are similar to those obtained on AM3 but are lower than on CMSX-11 and MC2. Further analysis has still to be carried out to explain these differences.

Microstructural stability

Subsurface microstructure The MC-NG alloy is sensitive to the precipitation of TCP phases in relation to its high content of refractory element like rhenium. The present study concerns the metallurgical characterization of these phases and their influence on the low-cycle fatigue properties. The SRZ is generated during coating processes with the formation of Ni-Al protective layer. The chemical diffusion at high temperature generates a needle-shape type P TCP phase in a γ' matrix. The thickness of this zone ranges from 5 to 40µm (Figure 8).

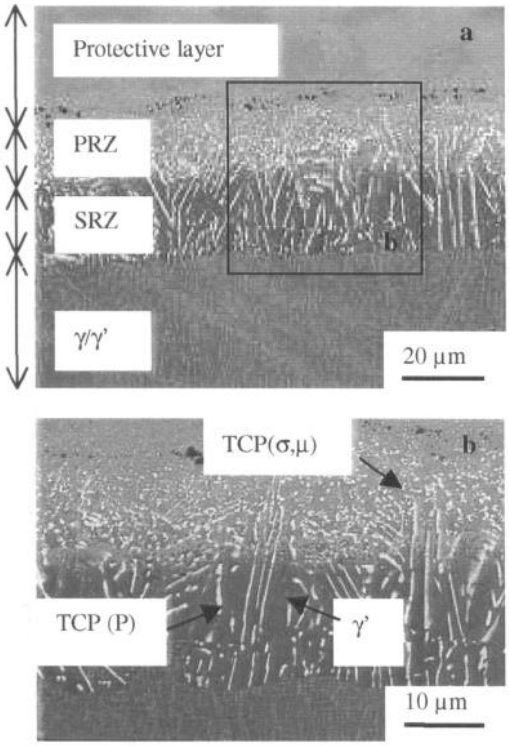

Figure 8: SRZ description (a) with detail (b).

The surface residual stresses have a catalytic effect on the SRZ development. This observation has already been detailed in reference [3]. The removal by an electrolytic polishing of a surface layer (a few microns thick) prevents the SRZ formation; an ageing treatment after coating generates the precipitation of TCP phases again but with a much slower kinetics.
To evaluate its impact on low cycle fatigue properties, several tests have been performed at 950°C and 1100°C on coated and uncoated MC-NG specimens (Table V).

Table V Comparison of MC-NG life of coated and uncoated MC-NG specimens

Coating	Temperature (°C)	Stress (MPa)	Cycles to failure
No	950	500	18622
No	950	500	14791
Yes	950	500	6150
Yes	950	500	9687
No	1100	300	4784
No	1100	300	3880
Yes	1100	300	2928

We observe that the fatigue life decreases by a factor 2 for the coated specimens. Two reasons can explain this decrease: the effect of the protective layer and/or the effect of SRZ alone. We have been able to prove that this difference is mainly related to the protective layer independently of SRZ formation. Indeed, if we compare the fatigue life of uncoated and coated MC-NG to that of uncoated and coated AM1 (where there is no SRZ formation) we obtain an equivalent reduction ratio (1.7). Thus it can be assumed that the SRZ alone does not have a detrimental effect on the fatigue properties at 950°C and 1100°C. Moreover the fatigue life remains acceptable with regard to the specifications of the MC-NG damage law (see § Identification and validation of the damage model).
Furthermore a protective coating has also been applied by Turbomeca with a diffusionless MCrAlY type layer. No TCP phase precipitation has been observed with this type of coating, which is consistent with the involved diffusion mechanism for SRZ generation.

Volume microstructure Several creep tests were also performed at 950°C - 1050°C and 1150°C to evaluate the MC-NG sensitivity to the volume TCP phase formation. The results show that a local coalescence of γ' precipitates is particularly pronounced with increasing temperature (rafting formation) but does not affect the creep life in comparison with other single crystals (see § Creep properties). Moreover no TCP phase precipitation has been observed for long time exposures of up to 1665 hours.

Component life prediction

In addition to these experimental studies, a specific original approach is implemented to use all these results for the design and life calculations of turbine blades in running conditions. This approach consists in determining constitutive equations which are introduced in finite element analysis codes for part life prediction [9-11]. The behaviour model allows us to describe:
- the existing relation between stresses and strains in elasto-viscoplastic conditions,
- the evolution of these mechanical properties related to a finite volume of blade submitted to an external complex loading.
Moreover a lifing model describes the damage evolution laws within the material versus time to exposure. The time integration of these equations allows us to predict the time to

failure for blades and vanes which are submitted to a complex loading with the interaction between fatigue, creep and environmental effects.

MC-NG constitutive equations

Hypothesis Constitutive equations link stress, strain and time. The model is based on the continuous medium mechanical theory. The material is assumed to be homogeneous on the volume element scale. In comparison to the volume element, the heterogeneity is too small, so that the microscopic behaviour is considered equivalent to the mean macroscopic behaviour.

Expression of constitutive equations To describe this behaviour, elastic and plastic strains are distinguished. The elastic strain is given by the Hooke relation whereas the plastic strain is given by the Onera model [9,10] using seven parameters. This law is labeled 'double viscosity' since it takes into account the material behaviour for fast and slow deformation rates (denoted respectively ε_{pr} and ε_{pl}). This is quite representative of monotonic tensile and creep loadings. So the proposed model is quite accurate to describe the dwell time effects which are observed during engine running. The expression of the law is given by the following equations:

$$\dot{\varepsilon}_{pr} = \left\langle \frac{|\sigma - X| - R}{Kr} \right\rangle^{nr} \qquad \dot{X} = C\left(a\,\dot{\varepsilon}_{pr} - X\,\dot{p} \right)$$

$$\dot{\varepsilon}_{pl} = \left(\frac{\sigma}{K_l} \right)^{nl} \qquad \dot{R} = 0 \qquad (1)$$

Ki and *ni* are respectively the consistency and the hardening parameters in relation to the strain rate and the temperature.
R is the isotropic hardening (homogeneous increasing of the elasticity domain in relation to the elastic strain).
X is the kinematic hardening (translation of the elasticity domain).
C and *a* relate to the derivative of *X* in relation to the time.

Identification and validation of the constitutive equations Tensile and fatigue tests at several temperatures were performed to identify the constitutive equation parameters. This method allows the determination of the parameters for each temperature. The parameter smoothing on all the temperature range is then obtained with a specific optimization software developed by the Ecole des Mines de Paris and the Ecole Normale Supérieure de Cachan (SiDoLo ™).
After optimization, the validation of the model is carried out with creep-fatigue tests at 950°C and 1050°C. Figures 9a and 9b show a rather good fit between MC-NG experimental data and simulation.

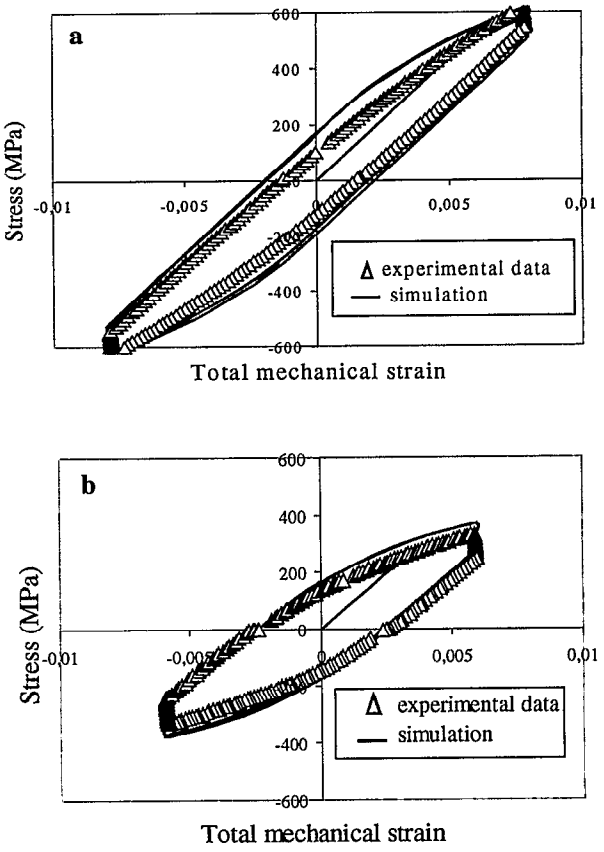

Figure 9: Comparison of MC-NG experimental data and simulation on creep-fatigue tests at 950°C (a) and 1050°C (b).

However, thermomechanical tests (cyclic strain and temperature) were performed to determine the limits of the model. This type of loading is more discriminating since it is closer to the actual engine running conditions [12].

MC-NG damage model

Hypothesis The absence of damage corresponds to a material free of cracking and cavity on the microscopic scale. The continuous damage theory describes the evolution between initiation and macroscopic cracking (a few millimeters). In the model we take into account:
- the fatigue damage (D_f) which is a function of the number of cycles,
- the creep damage (D_c) which is a function of the time.
Both damages are scalar values and can be added.
The environment effects are not directly considered, but are integrated within the D_c variable.

Expression of the damage model The expression of the damage model requires the knowledge of the parameter D. This parameter describes the material damage level. We consider it by introducing the effective stress concept:

$$\sigma_{eff} = \sigma/(1-D) \qquad (2)$$

The fatigue damage in anisothermal conditions is given by the Chaboche model [9] with the following equations:

$$\delta D_f = \left[1-(1-D)^{\beta+1}\right]^{\alpha}\left(\frac{\sigma_{max}-\bar{\sigma}}{M(1-D)}\right)^{\beta}\delta N \qquad (3)$$

With:
$$\begin{cases} M = M_0(1-b_1\bar{\sigma}) \\ \alpha = 1-a\left\langle\dfrac{\sigma_{max}-\sigma_l}{1-\sigma_{max}}\right\rangle \\ \sigma_l = \sigma_{l0}(1-b_2\sigma_{l0})+\bar{\sigma} \end{cases} \qquad (4)$$

The coefficients β, a, σ_{l0}, M_0, b_1 and b_2 are unique for a given material.
The Rabotnov model [11] describes the creep damage. Its expression is as follows:

$$\delta D_c = \left(\frac{\sigma}{A}\right)^{r}(1-D_c)^{-k}\delta t \qquad (5)$$

The coefficients A, r and k depend on the alloy and the temperature.
At high temperatures fatigue and creep damage can interact. To simulate this phenomenon we simply add the elementary damage values D_f and D_c. We therefore take into consideration the physical effects such as:
- the increasing of the fatigue crack propagation rate due to the creep cavities,
- the increasing of the creep cavities volume due to the concentration of stress at the crack tip.
This method leads to a non linear damage evolution which is well assessed by the experimental data.

Identification and validation of the damage model The identification of the damage model is based on several tensile, fatigue and creep tests. Up to now the number of tests performed on the MC-NG are not sufficient to identify all the parameters. However, some referring fatigue and creep tests (Figures 5 and 6) show that the MC-NG mean life is twice greater than that of the AM1. Therefore, in a first approach the damage model parameters were determined by using the AM1 curves with a factor 2 on the number of cycles or the time to failure.

Application of the constitutive equations and the damage model for the part life prediction

The life of a high pressure turbine blade of the M88 military engine (Figure 10) has been calculated with MC-NG behaviour and damage laws.

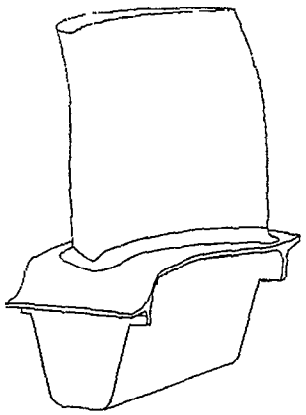

Figure 10: Design of a high pressure turbine blade of the M88 military engine.

The part life prediction method involves the following stages:
- 1D calculation using the elasto-viscoplastic behaviour established in the radial direction (direction <100> of the single crystal),
- stress calculation in different sections perpendicular to the blade axis,
- prediction of the number of cycles to failure using the damage model with the creep and fatigue interactions.
Then some overstress coefficients are locally applied to take into account:
- the disparity due to the anisotropy. This difference is determined by the comparison of 1D and 3D calculations which are performed in a localised area of the part,
- the stress concentrations due to the geometrical singularities, like holes.
The external loadings used in the numerical prediction are representative of an endurance cycle similar to the flying conditions. This complex cycle unites the temperature and stress variations. The results are presented for the critical section of the blade (Figure 11). The plotted factors represent the ratios between the MC-NG and AM1 number of cycles to failure. In this section the maximum temperature is 1050°C.

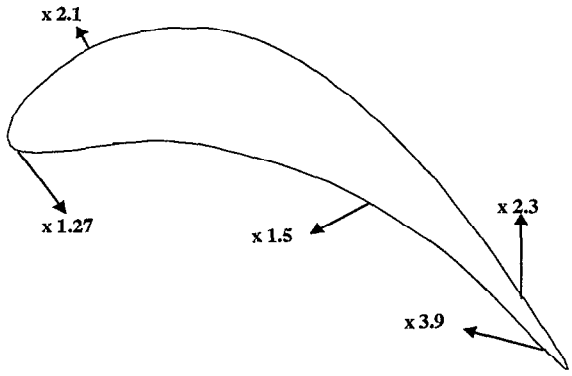

Figure 11: Predicted gain of life between AM1 and MC-NG for the same solicitations.

These results lead to the following remarks:
- in the creep predominant areas (with 950°C<T<1050°C) the MC-NG gain ranges between 1.3 and 2.1. In these conditions the MC-NG contribution is limited,
- in the fatigue predominant areas the gain ranges between 2.3 and 3.9. This is due to the more favourable behaviour of MC-NG as compared to AM1. In these conditions the stress relaxation is more important than for AM1.
The data analysis enables the modification of the blade shape to decrease the critical area solicitations. After design optimization for MC-NG, the life gain would be better than a factor 2 throughout the part compared to the AM1 blade.

Conclusion

This paper synthesizes the main basic works performed on the new generation single crystal MC-NG by Snecma and Turbomeca. It presents the different stages for the implementation of a new material which are the development, the characterization and the industrial design of parts. With its outstanding mechanical properties at high temperature and good environment resistance, MC-NG appears to be quite a valuable candidate for turbine blades in future turboshaft engines. This result is the consequence of a beneficial collaboration with the Onera research laboratory. Today Snecma and Turbomeca have produced some MC-NG blades for high pressure turbines. Both engine manufacturers will shortly test those parts on their experimental engines in very severe loading and temperature conditions. In parallel the evaluation of implementation processes (machining, brazing) and repairing is in progress.

Acknowledgements

The authors are grateful to the Service des Programmes Aéronautiques for their financial support of the MC-NG programme and acknowledge Laurence Potez, Alain Lyoret and Jean-Louis Ragot for their scientific participation in this research work.

References

1. P. Caron, "High γ' Solvus New Generation Nickel-Based Superalloys for Single Crystal Turbine Blade Applications" (Paper will be presented at the 9th International Symposium on Superalloys, Champion, Pennsylvania, 17-21 September 2000).

2. Philippe Perruchaut, Patrick Villechaise, and José Mendez, "Some Aspects of Environmental Effects on the Fatigue Damage of the AM1 Single Cristal Superalloy at High Temperature", Corrosion-Déformation Interactions (Nice, France: Thierry Magnin, 1996), 342.

3. W.S. Walston, J.C. Schaeffer and W.H. Murphy, "A New Type of Microstructural Instability in Superalloys – SRZ", Superalloys 1996, ed. R. D. Kissinger et al. (Warrendale, PA: The Minerals, Metals and Materials Society, 1996), 9-18.

4. W.S. Walston and al., "René N6: Third Generation Single Crystal Superalloy", Superalloys 1996, ed. R. D. Kissinger et al. (Warrendale, PA: The Minerals, Metals and Materials Society, 1996), 27-34.

5. David N. Duhl, Alloy Phase Stability and Design (Pittsburgh, PA: Materials Research Society, 1991), 389-399.

6. "Development and Turbine Engine Performance of Advanced Rhenium Containing Superalloys for Single Crystal and Directionnally Solidified Airfoils", Rhenium and Rhenium Alloys, ed. B. D. Bryskin (Warrendale, PA: The Minerals, Metals and Materials Society, 1997),731-754.

7. J. L. Smialek et al., "Effects of Hydrogen Annealing, Sulfur Segregation and Diffusion on the Cyclic Oxidation Resistance of Superalloys: a Review," Thin Solid Films, 253 (1994), 285-292.

8. Y. Zhang et al., "Synthesis and Cyclic Oxidation Behavior of a (Ni,Pt)Al Coating on a Desulfurized Ni-Based Superalloy", Metallurgical and Materials Transaction A, 30A (1999), 2679-2687.

9. Jean-Louis Chaboche, and Jean Lemaitre, Mécanique des Matériaux Solides (Paris, France: Dunod, 1985).

10. P. Poubanne, R. Krafft, and J. P. Mascarell, "Modélisation du Comportement Sous Sollicitation de Fluage Cyclique (Double Viscosité)" (Report YLEC 137/90, Snecma, 1990).

11. Y.N. Rabotnov, Creep Problem In Structural Members (North Holland Publishing Company, 1969).

12. J.Y. Guedou and Y. Honnorat, "Thermomechanical Fatigue of Turbo-Engine Blade Superalloys," Thermomechanical Fatigue Behavior of Materials, ed. Huseyin Sehitoglu (Philadelphia, PA: ASTM STP 1186, 1993),157-175.